GENETIC ALGORITHM-BASED HEAT TRANSFER ENHANCEMENT TECHNIQUE OF A PROTRUDED MICRO-CHANNEL

by

Ke YANG, Zhaoli ZHENG, and Di ZHANG*

Key Laboratory of Thermal-Fluid Science and Engineering, Xian Jiaotong University, Ministry of Education, Xian, China

Original scientific paper
https://doi.org/10.2298/TSCI180517087Y

As an innovative type of passive flow control structure, the protrusion exhibits great potential for heat transfer enhancement. In this paper, genetic algorithm is used for the dimensional optimization of a protruded micro-channel. The protruded micro-channel is studied at four mass-flow rates. In all the cases, thermal performance is selected as the objective function that represents both heat transfer and flow friction. The radius of the protrusion and the distance are selected as the two optimized parameters, and their ranges are decided by physical topologies. The objective function thermal performance is calculated by an auto-CFD batch program. The results shows that there are two peaks of thermal performance values when R and δ change in the cases with flow rates equaling $4 \cdot 10^{-5}$ kg/s and $6 \cdot 10^{-5}$ kg/s, while at the other two flow rates, the thermal performance values increase monotonously. The global optimal solutions for the four flow rates and two local optimal solutions are given in this research, and it is helpful to choose the best design variables to achieve the highest thermal performance. It also can be found that at all the different flow rates, the optimized shape of micro-channel has the same point that (R-δ) is nearly 45 μm in the studied ranges of optimized parameters.

Key words*: genetic algorithm, micro-channel, flow control structures*

Introduction

Heat transfer plays an important role in many modern industries, such as automotive, aerospace, integrated circuit, and cryogenic industries. It has been estimated that more than 80% of the energy utilization involves the heat transfer process [1]. As some researches show, the local power density of chips or some other high density integrated circuits has reached 300 W/cm^2 or higher [2], which inevitably brings out high heat flux for these electronic devices. Moreover, high efficient heat transfer cannot only save much energy during these process, but also can reduce the accident rates, especially in electronical devices, which are frequently supposed as serious problems due to overheat. Commonly, raising temperature by 10 K, the reliability of the electronic product will be reduced by half than the original value [3]. Thus, we need to find an optimal flow control structure. During the last few years, many flow control structures have been proposed to get better thermal performance (TP), such as dimples/protrusions [4, 5], corrugated plate [6], pin-fins [7, 8], inner V-grooves, ribs, *etc.* The investigations about fluid-flow and heat transfer characteristics in different channels have been studied separately in many aspects. Roth *et al.* [9] evaluated the heat transfer in straight silicon channels with

* Corresponding author, e-mail: zhang_di@mail.xjtu.edu.cn

integrated in-line and staggered pin-fin arrays at clearance to diameter ratios of 0.50-0.77 in the laminar flow regime at Reynolds numbers ranging from 9 to 246. The measurements showed that a significant portion of the fluid-flows below the pin fins in the clearance bypass region, leading to heat transfer results that show an improvement over an unfinned reference geometry. All these researches show that flow control structures can effectively enhance or influence heat transfer in the internal flow. In these different flow control structures, protrusion and pin-fin are the two flow control structures which have best TP in low Reynolds number [10], so protrusion is used as the flow control structure in this research. In another aspect, heat transfer efficient changes greatly with respect to physical dimensions of flow control structures in micro-channel. As for the optimization of physical dimensions of flow control structure, there are many researches have been done all around the world and most of these researches focus on the parameters of flow and heat transfer. Rao *et al.* [11] used a new proposed optimization algorithm named as *Jaya algorithm* to do the dimensional optimization of a micro-channel heat sink. The results obtained by the application of Jaya algorithm are found much better than TLBO algorithm [12] and a hybrid multi-objective evolutionary algorithm. Xie *et al.* [13] computational optimized the internal cooling passages of a guide vane by a gradient-based algorithm. Lin *et al.* [14] developed a combined optimization procedure to look for optimal design for a micro-channel heat sink. The geometry and flow rate distribution were considered for optimization. The optimization was proven effective only for the double-layer MCHS with a specific dimension.

Based on the foregoing reviews, it is observed that some of the researches [9, 10, 15, 16] had only involved different types of flow control structures without any optimization. Hence, it cannot show the best TP of each type of flow control structures. Some of the researchers [14, 17, 18] had considered only flow friction as the objective for optimization. This is not comprehensive for micro-channel heat sink, and some of the researchers use empirical or fitting formula such as response surface methodology (RSM), and then to take the extreme value as the optimal solution. This is not accurate enough. So in this study, an auto-CFD batch program is used to call some commercial software to solve every cases directly, and the dimensional optimization is done for the same type of flow control structure, and also, both heat transfer and flow friction are considered using a TP parameter in the optimization process.

Numerical methods

Governing equations and data reduction

Water with constant properties is considered as working fluid in this study, the conservation equations for mass, momentum, and energy are used to get the flow and thermal characteristics.

The Fanning friction factor, f, [19] is calculated and it is defined:

$$f = -\frac{\left(\frac{\Delta p}{L}\right) D_h}{2\rho U_{\text{ave}}^2} \tag{1}$$

The Nusselt number is defined as:

$$\text{Nu} = \frac{hD_h}{k} \tag{2}$$

where h is heat transfer coefficient, k – the fluid thermal conductivity. The h can be derived from:

$$h = \frac{q''}{\Delta T} \tag{3}$$

$$\Delta T = T_{w,\text{ave}} - T_{f,\text{ave}} \tag{4}$$

where q'' represents the heat flux, and ΔT – the average temperature difference between the wall and the fluids [3, 20, 21].

The whole TP factor considers both the heat transfer and the friction resistance, which is described as:

$$TP = \left(\frac{\text{Nu}}{\text{Nu}_0}\right)\left(\frac{f}{f_0}\right)^{-1/3} \tag{5}$$

Physical models and boundary conditions

A schematic diagram of the geometry and the computational domain is showed in fig. 1. In the micro-channel, the fluid-flow will develop into typical periodic flow structures after a certain flow distance. At this situation, only one periodic domain was considered with periodic boundary conditions applied at the inlet and outlet for the simulation. The original rectangular micro-channel is 50 μm (height) × 200 μm (width) in cross-section, and the periodic length is 150 μm. Protrusions, which can be regarded as passive flow control structures [22], are arranged on one external wall of the channel. The flow is fully developed with a fluid bulk temperature of 300 K, a uniform heat flux of $q'' = 5 \cdot 10^5$ W/m^2 and no-slip boundary conditions are specified at the external surfaces of the micro-channel.

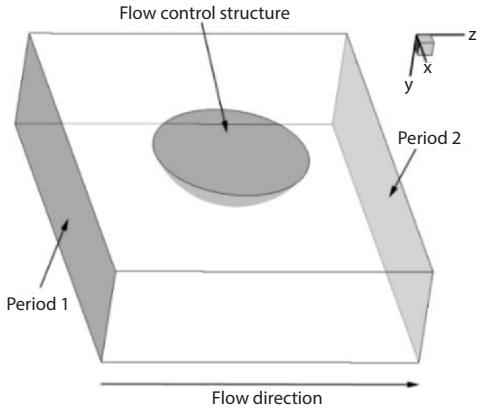

Figure 1. Schematic diagram of boundary conditions

The flow rate is set for the periodic boundary, flow rates $2 \cdot 10^{-5}$ kg/s, $4 \cdot 10^{-5}$ kg/s, $6 \cdot 10^{-5}$ kg/s, and $8 \cdot 10^{-5}$ kg/s are specified on the periodic inlet boundary automatically by the optimization main program.

The radius of protrusion, R, and the distance between sphere center and external wall, δ, are the two parameters optimized in this study. The lower range and upper range of these two parameters are shown in tab. 1. The negative value of δ means the sphere centre is located inside of the rectangle channel.

Table 1. Design variables and their ranges for the flow control structures

Design variable	Lower range [μm]	Upper range [μm]
R	10	60
δ	–10	20

Optimization methods

The TP of these studied cases is influenced by many parameters. Flow type and the number of vortices may change largely due to small changes of flow control structure size, and so to the TP. At this situation when a new vortex appears or flow separates from the flow control structures suddenly, TP may be discontinuous. So some approximation methods such as the RSM and pattern search algorithm [23, 24] are not appropriate in some occasions.

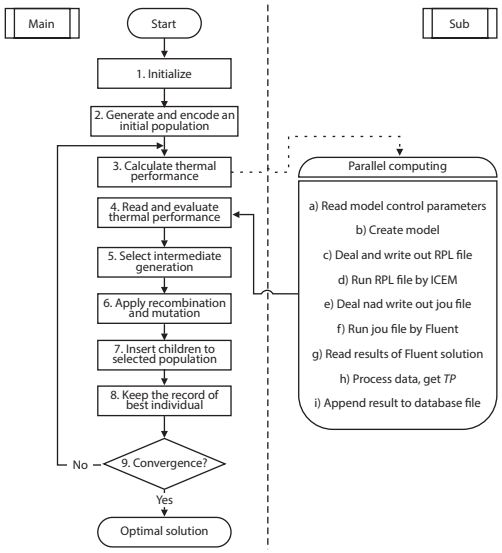

Figure 2. Flow chart of the main program

Table 2. Grid independence validation at the condition of kg/s

Case	Seed size	Nu	Difference [%]
1	5.0	2.9900	5.00
2	3.5	2.8493	1.76
3	2.0	2.7984	0.29
4	1.0	2.7903	–

The genetic algorithm (GA) is used to find the optimal flow control structure. This algorithm is often used as a global search method that does not need gradient information. An implementation of the GA main program is schematically shows as flow chart in fig. 2.

Model validation

The meshes that all have tetrahedral elements are generated for the physical model, and are refined in the near-wall regions where the gradients of variables are very high. The usage of tetrahedral elements is because this type of elements is convenient to be generated by ICEM automatically using RPL file by the software's playing scripts function. In another aspect, the physical models change greatly in different cases, so the block method to generate hexahedral elements is impractical. What's more, using a constant mesh number to control the mesh quality is not suitable when the model changes greatly. In this study, the global element seed size and global element scale factor are used to control the mesh size in all the cases. Table 2 shows three cases with different global element seed size that are used to generate meshes of physical model with equaling 50 μm and equaling 10 μm, and the relative difference of TP and Nusselt number is listed. The last case is used to generate meshes in the following study. Comparing with previous published results [10], Nusselt number difference is less than 1%, therefore, the proposed model could be used to simulate the flow and heat transfer characteristics in the micro-channel.

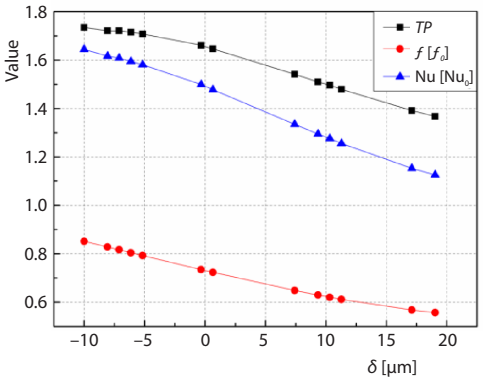

Figure 3. Variations of f/f_0, Nu/Nu_0 and TP with d at flow rate equalling kg/s

Results and discussion

Effect of the distance, δ, on the temperature and flow fields

Effect of the distance, δ, on heat transfer performance is analyzed. First of all, the results of flow rate equaling $2 \cdot 10^{-5}$ kg/s are calculated. At this flow rate, the optimization process is carried out three times to avoid local optimized solution. The total number of the cases which are simulated is 487. The results of the three times all reveal that the best solution is as:s, the highest thermal performance is 2.41 when R equals 52.85 μm and δ equals 8.91 μm. For detailed research, tab. 3 lists some of the cases with the

same protrusion radius. Figure 3 shows the variations of thermal parameters with δ at flow rate equaling $2 \cdot 10^{-5}$ kg/s. The temperature distribution on the protruded wall of these cases are shown in fig. 4, and also the temperature distribution and streamlines in the stream-wise middle sections are shown in fig. 5.

Table 3. The results of four cases with the same radius when varies

Case	R	δ	TP	f/f_0	Nu/Nu_0
250	29.05	–10.00	1.73	0.85	1.64
263	29.05	0.65	1.65	0.72	1.47
217	29.05	11.29	1.91	0.61	1.26
204	29.05	17.10	1.39	0.57	1.15

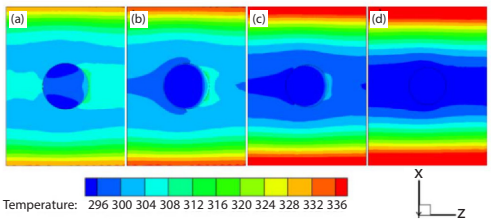

Figure 4 . Temperature distribution [K] on the structured walls; $Q = 2 \cdot 10^{-5}$ kg/s, (a) Case 250, (b) Case 263, (c) Case 217, and (d) Case 204

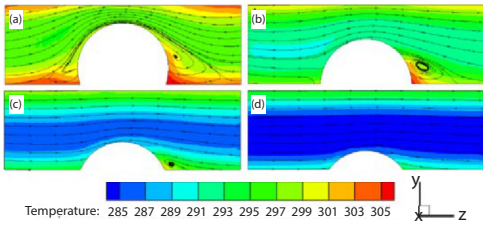

Figure 5. Temperature distribution [K] and streamlines in the stream-wise middle sections, Case: $Q = 2 \cdot 10^{-5}$ kg/s; (a) Case 250 (b) Case 263, (c) Case 217, and (d) Case 204

The distance, δ, is growing larger from figs. 5(a)-5(d), and from this pictures it can be easily found that temperature gradient becomes much larger as δ grows. In fig. 5(a), the fluid-flows into this channel and quickly impinges on the protrusion, flow separates near the trailing edge of the protrusion and reattaches quickly before next period. As the sphere center of protrusion goes along the outward direction of the rectangle channel, the vortices before the protrusion disappears gradually first, figs. 5(a)-5(c), and then the vortices near the trailing edge of the protrusion disappears when the sphere center moves further along the outward direction figs. 5(a)-(d). But in another aspect, the vortices has great benefit to the mixing of cold and hot fluid which is beneficial to convective heat transfer. So the heat dissipated in large δ cases are much larger. The average temperature of the structured wall changes slightly as the sphere center moves along the outward direction. But the temperature of the flow region decreases quickly when the sphere center moves along the outward direction, while, heat is mainly dissipated by the fluid which absorb heat from the external walls and take it out of the channel. So the higher the flow region temperature is, the more heat is dissipated.

In another aspect, flow friction also is a factor that influences the usage of micro-channels. Considering both tab. 3 and fig. 3, it can be found that the relative Fanning friction, f/f_0, increases with the increasing of δ. This is mainly because the throat opening area changes regularly with the moving of sphere center.

At last, the whole heat transfer performance is evaluated by TP, which considers both the heat transfer augmentation and the increase of friction loss [16]. The TP increases first when δ changes from –10 μm to 0.65 μm, and then decreases when δ increases from 0.65 μm to 11.29 μm , and again increases when increasing from 11.29 μm to 17.10 μm.

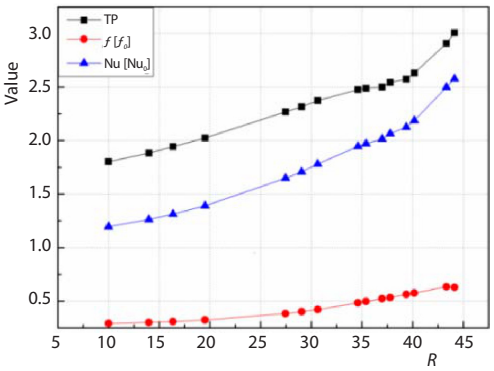

Figure 6. Variations of f/f_0, Nu/Nu_0, and TP with R [μm] at flow rate equaling kg/s

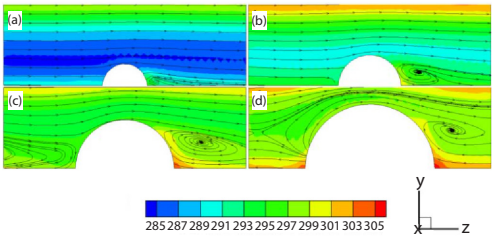

Figure 7. Temperature [K] distribution and streamlines in the stream-wise middle sections Case: $Q = 4\times10^{-5}$ kg/s; (a) $R = 13.97$, (b) $R = 19.52$, (c) $R = 30.63$, and (d) $R = 40.16$

Effect of the radius, R, on the temperature and flow fields

All the cases with the same distance, δ, when flow rate equals $4\cdot10^{-5}$ kg/s are analyzed in this section. After several times optimization, the total number of cases carried out in this flow rate is 911. Figure 6 shows the f/f_0, Nu/Nu_0, and TP variations with the changing of protrusion radius. It can be obviously observed that all these three parameters increase with the increasing of radius R. The maximum TP is reached at $R = 45$ μm when equals 0.65 μm.

Figure 7 shows the temperature distribution and streamlines on the stream-wise middle sections at flow rate equaling $4\cdot10^{-5}$ kg/s. The average temperature of the fluid domain raises up quickly with the increasing of protrusion radius. The Nu/Nu_0 is larger when protrusion grows bigger. Moreover, the temperature of the center region in Y-direction is lower than that near the external walls, which is just because the external walls are heated by a constant heat flux. But there also is a high temperature region near the trailing edge of the protrusion especially in the last three figures, figs. 7(b)-(d). Furthermore, when protrusion grows bigger individually, the positions of separatio and reattachment move along the anti-flow direction and flow direction, respectively, therefore, the separatio bubble grows larger gradually, figs. 7(a)-7(d). At last, the separatio bubbles almost fills the whole domain between the protrusions.

Optimization result

The final results are obtained and all the parameters including, R, δ, and TP are extracted from the simulation results. Table 4 lists these three parameters. It can be found that the $(R - \delta)$ is nearly 45 μm in all the four cases, which reveals that flow friction has little influence on the TP in this study. While the heat transfer has remarkable impact on TP, the increasing of Nu/Nu_0 makes higher TP in these cases.

The optimal solution of the four flow rates are all the same, and the detailed parameters are listed in tab. 4. While, in middle flow rates, there also are two local optimal solutions that can be get using GA.These two local optimal solutions have much smaller flow friction than the global optimal solutions, which may be useful at some special situations. While in the local optimal solutions, the sphere center is located inside the rectangle channel, this is much different from the cases studied by some other researchers [2, 3] while they use fixed sphere center and always put the sphere center out of the rectangle channel or on one of the external walls. Furthermore, it can be easily found that TP increases with the increasing of flow rate quickly, flow rate has much larger influence than the shape of flow control structures.

Table 4. Global and local optimal solutions for protruded micro-channel with different flow rates

$Q \cdot 10^{-5}$ [kgs^{-1}]	R [μm]	δ [μm]	TP
2	59.21	16.13	2.51
4	60.00	15.16	3.30
4	38.57	–6.13	3.20
6	60.00	16.13	4.22
6	37.78	–7.10	4.05
8	60.00	15.16	5.95

Figure 8 shows the temperature distribution of the global optimal solution at different flow rates. All of the four optimal solution has the similar shape. It can be found from the result that the more the protrusion cut into the rectangle channel, the higher TP can be get in the selected ranges for R and δ, which reveals that friction has much smaller influence on the value of TP in this study. Figure 9 shows the two local optimal solutions listed in tab. 4. The local optimal solution is a shape with smaller flow friction and lower heat transfer performance, which gets a lower peak before the R reaches the upper limit of its range. Considering both the local optimal solutions, figs. 9(a) and 9(b) and global optimal solutions, figs. 8(b) and 8(c), it can be found that the temperature gradient in the local optimal solutions is much larger. Because the value of TP has little difference, the maximum and minimum values of temperature in local optimal solution are larger and smaller than that in the global optimal solutions, respectively. Finally, the same as previously mentioned, these two local optimal solutions can be useful at some special situations when flow friction is limited exactly.

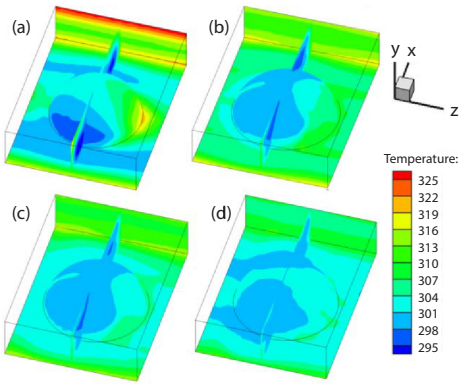

Figure 8. Temperature distribution of global optimal solutions; (a) $Q = 2 \cdot 10^{-5}$ kg/s, (b) $Q = 4 \cdot 10^{-5}$ kg/s, (c) $Q = 6 \cdot 10^{-5}$ kg/s, and (d) $Q = 8 \cdot 10^{-5}$ kg/s

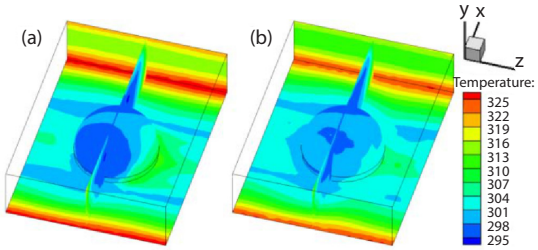

Figure 9. Temperature distribution of two local optimal solutions; (a) $Q = 4 \cdot 10^{-5}$ kg/s, (b) $Q = 6 \cdot 10^{-5}$ kg/s

Conclusions

In this research, dimensional optimization of a protruded micro-channel is done using the GA, the sphere radius of protrusion, R, and δ the distance between sphere center and external walls are the two parameters which are optimized, from which we can get the following conclusions.

- There are two peaks of TP values when R and δ changes in the cases with flow rates equalling $4 \cdot 10^{-5}$ kg/s and $6 \cdot 10^{-5}$ kg/s, which means TP increases firstly with the increasing of R and δ, and then decreases, after reach a local minimum value of TP, once again, it increases

with the increasing of R and δ. While at the other two flow rates, the values TP increases monotonously.

- The global optimal solutions for the four flow rates are given in tab. 4, which are helpful to choose the best design variables listed in this table to get the highest TP.
- There also shows two local optimal solutions in tab. 4, which can be used in some special situations when flow friction or pressure drop is exactly restricted.
- It can be found that in all the different flow rates, the optimized shape of micro-channel has the same point that ($R - \delta$) is nearly 45 μm, which means the more the protrusion cut into the rectangle channel, the higher TP can be get in the studied ranges of R and δ.

Nomenclature

D_h – hydraulic diameter, [m]
f – Fanning friction factor
k – thermal conductivity, [$Wm^{-1}K^{-1}$]
L – periodic length, [m]
Δp – pressure drop, [Pa]
Q – mass-flow rate, [kgm^{-1}]
q'' – heat flux, [Wm^{-2}]
R – radius of protrusion, [m]
U – velocity in flow direction, [ms^{-1}]

Greek symbols

δ – distance, [m]
ρ – fluid density [kgm^{-3}]

References

[1] Chen, Q., *et al*., Optimization Principles for Convective Heat Transfer, *Energy*, *34* (2009), 9, pp. 1199-1206
[2] Shen, H., *et al*., Computational Optimization of Counter-Flow Double-Layered Micro-Channel Heat Sinks Subjected to Thermal Resistance and Pumping Power, *Applied Thermal Engineering*, *121* (2017), July, 5, pp. 180-189
[3] Xie, G., *et al*., Parametric Study on Thermal Performance of Micro-Channel Heat Sinks with Internal Vertical Y-Shaped Bifurcations, *International Journal of Heat & Mass Transfer*, *90* (2015), Nov., pp. 948-958
[4] Li, P., *et al*., Laminar Flow and Forced Convective Heat Transfer of Shear-Thinning Power-Law Fluids in Dimpled and Protruded Micro-Channels, *International Journal of Heat & Mass Transfer*, *99* (2016), 5, pp. 372-382
[5] Zhang, D., *et al*., An Experimental Study on Heat Transfer Enhancement of Non-Newtonian Fluid in a Rectangular Channel With Dimples/Protrusions, *Journal of Electronic Packaging*, *136* (2014), 2, pp. 021005-021005-021010
[6] Naphon, P., Kornkumjayrit, K., Numerical Analysis on the Fluid-Flow and Heat Transfer in the Channel with V-Shaped Wavy Lower Plate, *International Communications in Heat & Mass Transfer*, *35* (2008), 7, pp. 839-843
[7] Liu, M., *et al*., Experimental Study on Liquid-Flow and Heat Transfer in Micro Square Pin Fin Heat Sink, *International Journal of Heat & Mass Transfer*, *54* (2011), 25-26, pp. 5602-5611
[8] Yang, Y. T., Peng, H. S., Numerical Study of Pin-Fin Heat Sink with Un-Uniform Fin Height Design, *International Journal of Heat & Mass Transfer*, *51* (2008), 19-20, pp. 4788-4796
[9] Roth, R., *et al*., Heat Transfer in Freestanding Micro-Channels with in-Line and Staggered Pin Fin Structures with Clearance, *International Journal of Heat & Mass Transfer*, *67* (2013), Dec., pp. 1-15
[10] Yang, K.,*et al*., Heat Transfer and Entropy Generatio of Non-Newtonian Laminar Flow in Micro-Channels with Four Flow Control Structures, *Entropy*, *18* (2016), 8, 302
[11] Rao, R. V., *et al*., Dimensional Optimization of a Micro-Channel Heat Sink Using Jaya Algorithm, *Applied Thermal Engineering*, *103* (2016), June, pp. 572-582
[12] Rao, R.V., *et al*.,Teaching-Learning-Based Optimization: A Novel Method for Constrained Mechanical Design Optimization Problems, *Computer-Aided Design*, *43* (2011), 3, pp. 303-315
[13] Xie, G., *et al*., Computational Optimization of the Internal Cooling Passages of a Guide Vane by a Gradient-Based Algorithm, *Numerical Heat Transfer*, *69* (2016), 12, pp. 1311-1331
[14] Lin, L., *et al*., Optimization of Geometry and Flow Rate Distribution for Double-Layer Micro-Channel Heat Sink, *International Journal of Thermal Sciences*, *78* (2014), Apr., pp. 158-168
[15] Li Y., *et al*., Flow Development in Curved Rectangular Ducts with Continuously Varying Curvature, *Experimental Thermal & Fluid Science*, *75* (2016), July, pp. 1-15

[16] Liu, J., *et al*., Turbulent Flow and Heat Transfer Enhancement in Rectangular Channels with Novel Cylindrical Grooves, *International Journal of Heat & Mass Transfer*, *81* (2015), Feb., pp. 563-577
[17] Yang, Y. T., *et al*., Optimization Design of Micro-Channel Heat Sink Using Nanofluid by Numerical Simulation Coupled with Genetic Algorithm, *International Communications in Heat and Mass Transfer*, *72* (2016), Mar., 7, pp. 29-38
[18] Wang, X. D., *et al*., AnInverse Geometric for Geometry of Nanofluid-Cooled Micro-Channel Heat Sink, *Applied Thermal Engineering*, *55* (2013), 1-2, pp. 87-94
[19] Zhang, D., *et al*., An Experimental Study on Heat Transfer Enhancement of Non-Newtonian Fluid in a Rectangular Channel with Dimples/Protrusions, *Journal of Electronic Packaging*, *136* (2014), Apr., pp. 682-694
[20] Liu, J., *et al*., Numerical Modelling Flow and Heat Transfer in Dimpled Cooling Channels with Secondary Hemispherical Protrusions, *Energy*, *79* (2014), Jan., pp. 1-19
[21] Xie, G., *et al*., Turbulent Flow Characteristics and Heat Transfer Enhancement in a Rectangular Channel with Elliptical Cylinders and Protrusions of Various Heights, *Numerical Heat Transfer Application*s, *72* (2017), Oct., pp. 1-16
[22] Hur, D. S., *et al.* A Numerical Study on Flow Control Structure of a New-Type Submerged Breakwat *Journal of Korean Society of Coastal and Ocean Engineers*, *22* (2010), 3, pp. 181-190
[23] Abramson, M. A., Mixed Variable Optimization of a Load-Bearing Thermal Insulation System Using a Filter Pattern Search Algorithm, *Optimization and Engineering*, *5* (2004), 2, pp. 157-177
[24] Wetter, M., Polak, E., Building Design Optimization Using a Convergent Pattern Search Algorithm with Adaptive Precision Simulations, *Energy & Buildings*, *37* (2005), 6, pp. 603-612

Paper submitted: May 17, 2018
Paper revised: August 23, 2018
Paper accepted: November 6, 2018